

# Clinical Outcomes of a New Enhanced Depth of Focus Intraocular Lenses

**Bartłomiej Markuszewski<sup>1,2\*</sup>, Adam Wylegala<sup>1,4</sup>, Kaja Bator<sup>2</sup>, Magdalena Kijonka<sup>1,3</sup>, Magdalena Nandzik<sup>1,3</sup>, Anna Markuszewska<sup>2</sup> and Edward Wylegala<sup>1,3</sup>**

<sup>1</sup>Department of Ophthalmology, District Railway Hospital in Katowice, Medical University of Silesia, Panewnicka 65, 40-760 Katowice, Poland

<sup>2</sup>Wrocławskie Centrum Okulistyczne, Zakładowa 11, 50-231 Wrocław, Poland

<sup>3</sup>Department of Ophthalmology, Faculty of Medical Sciences, Zabrze, Medical University of Silesia, 40-760 Katowice, Poland

<sup>4</sup>Experimental Ophthalmology Unit, Department of Biophysics, Silesian Medical University, Panewnicka 65, 40-760 Katowice, Poland

## \*Corresponding author

Bartłomiej Markuszewski, Department of Ophthalmology, District Railway Hospital in Katowice, Medical University of Silesia, Panewnicka 65, 40-760 Katowice, Poland.

**Received:** December 27, 2025; **Accepted:** January 05, 2026; **Published:** January 12, 2026

## ABSTRACT

**Purpose:** To demonstrate the results of ray tracing aberrometric measurements and optical function of recently introduced enhanced depth of focus intraocular lenses.

**Methods:** Lower and higher-order aberrations, refraction, distance and near visual acuity, and tear break-up time were measured at scotopic pupil size in 121 eyes of patients who received either the Vivity lens (Alcon AcrySof IQ Vivity) or the LuxSmart lens (Bausch + Lomb LuxSmartTM). Measurements were obtained using ray tracing aberrometry, with corneal placido topographic subtraction to delineate internal aberrations.

**Results:** The application of the Kefft algorithm to the empirical material for both types of extended depth of focus lenses allowed to determine the quality symbol by obtaining estimators of individual features of aberrations induced by each lens. The results of the comparison of the mean quality level coefficient showed no statistically significant difference between the lenses in terms of lens induced aberrations  $p=0.127$  and total ocular aberrations without defocus  $p=0.288$  and following defocus correction.

**Conclusion:** Both extended depth of focus intraocular lens models effectively achieved refractive targets for distance and near vision, with similar high-order aberrations.

**Keywords:** Aberrometry, Extended Depth of Focus, Kefft, Refractive Surgery, Lens Surgery

## Introduction

Advanced premium intraocular lenses (IOLs), such as multifocal and Extended Depth of Focus (EDoF) IOLs, offer the promise of clear vision across various ranges, potentially eliminating the need for glasses or significantly decreasing dependence on glasses after cataract surgery or refractive lens exchange [1-7]. The aim is to restore vision quickly and precisely, achieving satisfactory uncorrected vision at most distances. Optical aberrations, which deviate from the ideal wavefront, are categorized into lower-order aberrations (like basic refractive errors) and higher-order

aberrations (HOAs) such as spherical aberration and coma, which can significantly affect visual quality [8] and are not corrected by standard glasses or contacts. Light scattering, along with HOAs, can degrade image clarity on the retina [9]. The level of optical aberrations varies based on the IOL's design, especially the level of near vision enhancement. While there's no consensus on the effectiveness of aberrometers for evaluating multifocal IOLs' clinical performance [10-12], they can comprehensively describe the optical performance of the pseudophakic eye [13]. This study aimed to evaluate and compare the visual quality, refraction accuracy, and aberrometric results of two advanced non-diffractive EDoF IOLs.

**Citation:** Bartłomiej Markuszewski, Adam Wylegala, Kaja Bator, Magdalena Kijonka, Magdalena Nandzik, et al. Clinical Outcomes of a New Enhanced Depth of Focus Intraocular Lenses. *J Opto Opt Res*. 2026. 1(1): 1-8. DOI: doi.org/10.61440/JOOR.2026.v2.02

## Materials and Methods

The present prospective analysis was designed to assess and compare the functional visual outcomes post-cataract extraction with the implantation of two distinct types of IOLs: the Alcon Vivity (Vivity) and the Bausch & Lomb LuxSmart (LuxSmart). The study's scope extended beyond the basic evaluation of visual acuity, encompassing a comprehensive analysis of optical system parameters.

A key component of our assessment involved a detailed examination of the wavefront aberrations of the complete optical system. This analysis was conducted in accordance with Zernike's polynomial decomposition, both prior to and following the application of Defocus correction, a method commonly referred to as ocular wavefront optimization.

Further refinement in our analysis was achieved by isolating the contributions of aberration-inducing structures. Specifically, we quantified intraocular aberrations that manifest subsequent to the subtraction of corneal wavefront errors, thereby isolating the optical imperfections attributable to the IOLs themselves. Conversely, corneal aberrations were evaluated after excluding the influence of intraocular lens-induced aberrations, thus focusing on the corneal contribution to the overall wavefront error in both groups.

Through this bifurcated approach, the study aimed to discern the relative contributions of corneal and IOL-induced aberrations to the postoperative optical quality. Our methodology provides a nuanced understanding of the aberration profile associated with each IOL type, thereby informing clinicians in the selection of the most appropriate lens to optimize visual outcomes for patients undergoing cataract surgery.

This study was conducted in accordance with the principles outlined in the Declaration of Helsinki and received approval from the local bioethical committee (registration number 6/PNDR/2021). Informed consent was waived, as the study fulfilled regulatory and ethical criteria for minimal risk, meaning that participation did not expose subjects to risks or burdens beyond those encountered in routine clinical care, and thus met the requirements for a waiver of consent as recognized by federal regulations and discussed in the medical literature [14-17]. This approach is consistent with current ethical standards, which permit waivers of informed consent for research activities that pose no more than minimal risk to participants and do not adversely affect their rights and welfare [17].

## Characteristics of the Sample

The sample under investigation comprised a cohort of  $N = 64$  patients who underwent phacoemulsification with the implantation of advanced intraocular lenses (IOLs), specifically the Vivity (Alcon AcrySof IQ Vivity) and the LuxSmart (Bausch + Lomb LuxSmartTM), from 2021 to 2024. A total of 64 patients were selected for the empirical material, including 41 women and 23 men, aged between 34 and 81 years, who underwent cataract surgery and received EDOF lenses. Although there are nearly twice as many women as men, their average age is around  $59 \pm 11$  years, as illustrated in Table 1.

**Table 1: Characteristics of the Operated Patients by Gender and Age.**

Feature	Age				p test result
	Sex	N	Min	mean $\pm$ SD	
Female	Female	41	34	$59,2 \pm 10,7$	81
Male	Male	23	38	$59,0 \pm 10,5$	79
Total		64	34	$59,2 \pm 10,6$	81

There were 64 patients who received the same type of EDOF lens in both eyes. Of these, 34 patients were implanted with VIVITY-type EDOF lenses (see Table 2), while the remaining 30 patients received LUXSMART-type lenses. Their distribution by gender is homogeneous, as confirmed by the results in Table 3.

**Table 2: Characteristics of the Operated Patients Based on the Type of EDOF Lens Implanted in the Left and Right Eyes.**

Eye	EDOF lens type		Total	p test result
	VIVITY	LUXSMART		
Left	34	28	62	0,900
Right	34	25	59	
Total	68	53	121	

**Table 3: Characteristics of the Operated Patients by Gender and the Type of EDOF Lens Used.**

Sex	EDOF lens type		Total	p test result
	VIVITY	LUXSMART		
Female	44	33	77	0,931
Male	24	20	44	
Total	68	53	121	

The criteria for surgery qualification included a clinical or elective indication for cataract surgery, ranging from incipient to advanced stages, for presbyopia patients aiming for independence from spectacles. The exclusion criteria for the analysis were the presence of ocular disease, such as corneal dystrophy, maculopathy, glaucoma and ocular surface disease. All patients were admitted for outpatient cataract procedure at the Wrocław Ophthalmology Center, Wrocław, Poland. All surgical procedures were performed by a single surgeon (Dr. B.M.).

## Preoperative Assessment

All patients underwent pre-operative examination which consisted of: anterior and posterior segment examination via direct and indirect ophthalmoscopy, intraocular pressure test with air puff automated tonometer Canon TX-20 (Canon Inc. Tokyo, Japan), refraction examination with autokeratometer Canon RK-F2 (Canon Inc. Tokyo, Japan), distance visual acuity examination in logMAR scale in photopic conditions at 6 meters, near visual acuity at 40 cm, biometry using ACE (Bausch + Lomb, Laval, Canada – produced on license from Anterior Heidelberg Engineering, Heidelberg, Germany) and Tomey OA2000 (Tomey Corporation, Nagoya, Japan). The implant power for the previously myopic, emmetropic and hyperopic eyes was selected, targeting between emmetropia to  $-0.35$  Dpt. postoperative refractive power. A constant of 119.08 for Alcon

Vivity lens was used (optimized from 119.2) for the Universal Barrett II formula and 118.35 for the Bausch Lomb LuxSmart lens (optimized from 118.5) for the same Universal Barrett II formula.

### Intraocular Lenses

In this study, patients received an enhanced depth of focus Vivity lens and LuxSmart lens with combination of spherical aberrations allowing for depth of focus extention in order to provide distance, intermediate and some near spectacle free function, in both spherical and toric version.

The Alcon AcrySof IQ Vivity is a single-piece, hydrophobic acrylic lens with a 13.0 mm diameter and a 6.0 mm optic. It has a low refractive index and Abbe number, implying clear optics and minimal chromatic dispersion. Featuring advanced technology, it uses a non-diffractive approach to extend vision, including intermediate distances. Its aspheric design corrects for corneal spherical aberration. A central zone with dual transitional elements elongates and redirects the wavefront, optimizing the use of light for an extended depth of field, combining aspherical and spherical lens surfaces to improve the visual range [15].

The LuxSmart (Bausch + Lomb LuxSmartTM) IOLs are designed to extend depth of focus by controlling spherical aberration. They feature an aspheric design with a central zone of high power that transitions to a lower power at the edges, forming an Extended Depth of Focus (EDoF) channel for optimal possible focus. The design comprises different zones that direct light to focus at varying points, which can cause visual disturbances if not aligned correctly, similarly as in the Vivity lens. These 10.0 mm hydrophobic acrylic lenses have a 6.0 mm optic zone and come with or without a violet light filter. Utilizing 4th order spherical aberration to enhance the depth of field, the LuxSmart lens has shown to exhibit a defocus curve that can provide distance, intermediate and functional near vision [18].

### Surgical Technique

All patients underwent a standard, uneventful phacoemulsification surgery performed by one ophthalmic surgeon with 15 years of surgical experience. Anesthesia was administered via a topical proxymethacaine drip and intraocular lidocaine. Pupils were dilated with tropicamide and phenylephrine solutions. The Vivity lens was inserted using the Monarch injector, and the LuxSmart lens with the Medicel Accuject Pro injector, both through a 2.2 mm clear corneal incision. IOL alignment was aided by horizontal reference marks made at the corneal limbus prior to surgery when patients were upright, ensuring the patient's head was level with the slit lamp beam. Standard pre and postoperative care involved applying levofloxacin and 0.1% dexamethasone drops.

### Examination

Three months after surgery, patients underwent a thorough evaluation performed by one of three team examiners including uncorrected distance visual acuity (UDVA) and best-corrected distance visual acuity (CDVA), gauged using logMAR scale liquid crystal display charts at 6m. Near visual acuity (uncorrected and corrected) was also tested at 40 cm with Snellen

charts converted to logMAR. Tear break-up time (T.BUT) was measured to assess tear film quality due to its influence on visual quality with intraocular lenses, using fluorescein dye and averaging three readings.

Routine eye exams measured refractive error and intraocular pressure, and included ocular biomicroscopy and fundus examinations. Aberrometric and refractive data were obtained using the iTrace aberrometer (Tracey Technologies) which scans the eye via near-infrared to assess aberrations. Measurements were taken in a scotopic room light with the illuminance level of 450 lux, with unaltered physiological pupils and a visual target set at optical infinity, capturing data swiftly in under 200 milliseconds.

The iTrace system combines a Placido-based topographer for corneal wavefront errors and a ray tracing aberrometer for full eye aberrations. It also calculates the spherical equivalent refraction (SEQ) and detail low-order aberrations such as Defocus and Astigmatism, high-order aberrations such as Coma (including both vertical and horizontal, notated as Z3-1 and Z3+1, respectively), Trefoil (both vertical and oblique, notated as Z3-3 and Z3+3) and Primary Spherical Aberration (Z4^0), providing a comprehensive delineation of the optical components of the eye. The ray-tracing technology utilizes a serial, double-pass forward projections of narrow laser beam directed into the eye parallel to the line of sight by the means of x-y scanner, which moves the beam to cover the whole pupil area. Ocular aberrations result in a shift in the focus of the retinal image captured by a linear array of photoreceptors [19]. The paths taken by the light beams as the enter and exit enable the reconstruction of the actual wavefront error. This technology is less influenced by multifocal design of lenses as shown by Jun et al. [20].

The other aberrometry principle involves a parallel, double pass method using backward projections of a narrow laser beam sent along the visual axis that reflects on the retina, known as Hartmann-Shack Method. The outgoing light is directed through a series of relay lenses that project the pupil plane onto an array of small lenses, which divide the wavefront into multiple individually focused spots on a charge-coupled device (CCD) camera. The wavefront slopes are calculated by analyzing the displacement of the spots caused by the focal shift [21]. Charman et al. [22] described importance of identifying erratic measurements particularly for diffractive multifocal lenses but also in the refractive lenses.

The Tschnering principle is a parallel, double-pass technique that utilizes forward projection. In this approach, a broad laser beam passes through a screen with numerous round holes, creating a series of laser beams that enter the eye. A lens system permits the analysis of the retinal spot pattern for wavefront assessment. These types of aberrometers deliver consistent measurements in normal eyes but encounter limitations in eyes with significant aberrations due to spot overlap [23].

A new generation of aberrometers has been developed to assess ocular aberrations using Pyramidal Wavefront Sensor (PWS) technology, which is based on the Foucault knife-edge test

(Osiris, Costruzione Strumenti Oftalmici (CSO), Florence, Italy). In a pyramidal aberrometry system, a four-faced PWS captures wavefront gradients in two orthogonal directions, distributing four sub-pupils according to their intensity. Each sub-pupil implements a Foucault knife-edge test to determine the slope and shape of the wavefront. Unlike other methods, this approach samples the wavefront at the final stage of the optical path. A Hartmann-Shack (H-S) aberrometer, in contrast, discretizes the wavefront during the lenslet stage, and the number of measured samples is dependent on the number of lenses in the array. Typically, an H-S sensor contains 1000–2000 lenses with a resolution range of 250–1250  $\mu\text{m}$ , whereas the Osiris system samples with up to 45,000 points at maximum pupil dilation, corresponding to a resolution of 41  $\mu\text{m}$  [24].

### Statistical Analysis - Krefft Method

The method of measuring directly unmeasurable phenomena according to Krefft, with numerous applications in economics, medicine, dentistry and veterinary medicine, is a statistical model that allows, on the basis of empirical material collected from  $n$  patients for the number of  $k$  random variables (diagnostic features) in the model for  $k < n$ , to determine a directly unmeasurable synthetic function with a normal distribution describing the state of the examined phenomenon with a specific error  $\phi^2$  [25, 26]. In this work, we call this function for 7 variables the EDOF lens quality level (ZPJS).

The model of the function describing the quality level of EDOF lenses is a linear model and is expressed by the formula:

$$Y = \beta_0 + \beta_1 X_1 + \beta_2 X_2 + \dots + \beta_7 X_7 + \xi, \quad (1)$$

where:

- $Y$  – a synthetic variable explaining the quality level of EDOF lenses;
- $X_1, X_2, X_3, \dots, X_7$  – variables (diagnostic features) describing the severity of inflammatory changes in the vascular endothelium;
- $\beta_0, \beta_1, \dots, \beta_7$  – parameters (characteristics) of the model (1);
- $\xi$  – random component.

The linearity of the model is justified by the fact that the variable  $Y$  is a random variable, conditioned by the values of many variables, which are most often aggregated, i.e. interconnected, and therefore it can be assumed that the distribution of such a variable is at least asymptotically normal.

In order to statistically identify the model (1), i.e., to determine the values of the parameter estimators  $\beta_0, \beta_1, \dots, \beta_7$  with a specific degree of fit of the obtained model to the empirical data, it is sufficient to have experimental material in the form of measurements of 7 diagnostic features  $X_1, X_2, X_3, \dots, X_7$  from at least 10 patients, as well as information about the “directions of influence” of each of these diagnostic features on the quality level of the EDOF lenses in the model.

For the  $i$ -th random variable  $X_i$ , we say that it has a “positive influence direction” with respect to the variable  $Y$  — the quality level of EDOF lenses — denoted by the “+” sign, if an increase in the value of this variable favors an increase in the value of

variable  $Y$ , while it has a “negative influence direction,” denoted by the “-” sign, when its increase favors a decrease in the state of variable  $Y$ . Information about the “influence directions” of the individual 7 diagnostic features on the quality level of EDOF lenses in the model is integral knowledge of the researcher, based on their experience.

The A. Krefft algorithm allows for the generation of a vector  $\hat{Y}$  with a normal distribution in such a way that each component of the vector accounts, first, for the relationships between the individual diagnostic variables and variable  $Y$ , and second, that each component of variable  $Y$  simultaneously considers the interrelations between the diagnostic variables. This way, we obtain a model for the variable  $Y$  in the following form:

$$\hat{Y} = b_0 + b_1 X_1 + b_2 X_2 + \dots + b_7 X_7 \quad (2)$$

Given a known vector  $b$  with components  $b_0, b_1, b_2, \dots, b_7$ , for each set of diagnostic feature measurements  $X_{j1}, X_{j2}, \dots, X_{j7}$  of the  $j$ -th patient, the value  $\hat{y}_i$  is obtained. Furthermore, in order to use a more convenient scale for the synthetic variable than the scale of values  $\hat{Y}$ , a transformation from the scale of values  $\hat{Y}$  to the scale of values  $Z$ , in the form of the interval (0,1), is introduced using the following formula

$$Z = \frac{e^{\hat{y}}}{1 + e^{\hat{y}}} \quad (3)$$

where the letter  $e$  (Euler's constant) denotes the base of natural logarithms,  $e \approx 2.78$ .

It should also be noted that the obtained model (2) is subject to verification in terms of the fit of the values  $\hat{Y}$  obtained according to the model to the actual data. The fit index  $\phi^2$  values for individual models can only lie within the range {0 - 1}, so the closer the value of the index  $\phi^2$  is to zero, the more accurately the model describes the synthetic variable in question. Therefore, we refer to it as the method's error and can express it as a percentage.

## Results

### Empirical Material

The empirical material consists of measurements from 64 patients with an average age of  $59.2 \pm 10.6$  years, ranging from 34 to 81 years, who underwent cataract surgery and received an EDOF lens of the VIVITY or LUXSMART type. The empirical material includes measurements of the following 7 diagnostic features:

- X1: Total eye RMS
- X2: Low order total aberrations
- X3: High order total aberrations
- X5: Coma
- X8: Astigmatism
- X10: Trefoil
- X12: Secondary astigmatism

For both types of EDOF lenses, divided into 4 types of measured aberrations: F – without optical correction of defocus, C – with optical correction of defocus, Z – with subtracted corneal structure aberrations, N – aberrations resulting from the corneal structure.

The actual measurement values of these features in the model were rescaled to total values, and it was assumed – due to the fact that the smaller the aberrations, the higher the quality of the EDOF lenses – that there are 7 negative directions of influence of these features on the quality level of the EDOF lenses, marked with the “–” sign, which are presented in Table 1.

F5	-0,3026	-0,4675	STAT	-
F8	-0,3052	-0,6552	STAT	-
F10	-0,2996	-0,6356	STAT	-
F12	-0,4573	-0,4478	STAT	-
Intercept	12,2678			

### Model Identification

The application of the Kefft algorithm to the empirical material for both types of EDOF lenses without optical defocus correction allowed for the identification of model (2) with a fitting error of  $\phi^2 = 0.9012\%$ , in the following form:

$$\hat{Y} = b_0 + b_1 \cdot \ln(F_1 + 1) + b_2 \cdot \ln(F_2 + 1) + \dots + b_7 \cdot \ln(F_{12} + 1) \quad (4)$$

where  $F_i, i = 1, 2, \dots, 12$  are diagnostic variables describing the quality level of EDOF lenses.

The vector  $b$  with components  $b_0, b^1, b_2, \dots, b_7$ , with values compiled in Table 1, is the estimator of the parameters  $\beta_0, \beta_1, \dots, \beta_7$  of model (1), while the quality level of the EDOF lenses, measured on a scale from 0 to 1, is determined from formula (3) and denoted by the symbol  $Z_{PJS}$ .

In this model, we obtain the weights (estimators) of individual features by measuring the correlation coefficient of each of the 7 diagnostic features with the variable  $\hat{Y}$ , the quality level of the EDOF lenses, which appears in formula (4). The statistically verified values of these weights are presented in Table 4 and illustrated in Figure 1.

**Table 4: Estimators of the  $\beta$  Model Parameters, Weights, and Directions of Influence of the 7 Diagnostic Features Describing the Quality Level of EDOF Lenses Without Correction ( $Z_{PJS}$ ); STAT Indicates that the Given Weight Differs Significantly from Zero at the Level of  $p \leq 0.05$ .**

Variable	Components of vector $b$	Weight	Test result	Directions of influence
F1	-0,797	-0,7653	STAT	-
F2	-0,1269	-0,5555	STAT	-
F3	-0,4456	-0,8513	STAT	-

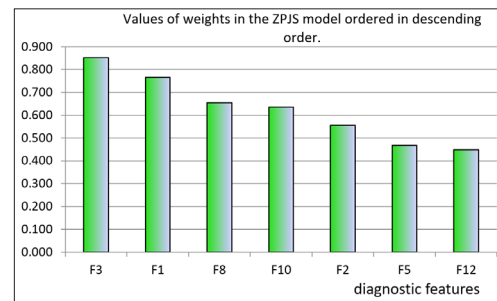


**Figure 1: Diagnostic Features Ordered by Weights Describing the ZPJS Quality Level of EDOF Lenses.**

It should be noted that the values of the weight estimators in the diagnostic feature model have signs consistent with their directions of influence on  $Z_{PJS}$  – the quality level of EDOF lenses. The greater the absolute value of the weight estimator for a given diagnostic feature, the stronger its association with ZPJS – the quality level of EDOF lenses. Thus, the features:  $F_3$  - High-order total aberrations,  $F_1$  - Total eye RMS, have the greatest influence on  $Z_{PJS}$  – the quality level of EDOF lenses, while the smallest influence is exerted by the diagnostic feature  $F_{12}$  – Secondary astigmatism. The range of correlation coefficients for these features with the diagnostic variable  $Z_{PJS}$  is between 0.45 and 0.85. This is because the diagnostic features describing  $Z_{PJS}$  – the quality level of EDOF lenses – are aggregated, meaning they are strongly interconnected, especially features  $F_1$  to  $F_2$  and  $F_8$ , as illustrated in Table 5. Moreover, they are collinear or nearly collinear.

**Table 5: Correlation Coefficients Between the 7 Diagnostic Features Describing  $Z_{PJS}$  – the quality level of lenses (upper triangle). An Empty cell is Equivalent to a Zero Value. Levels of Significance  $p$ , Indicating that a Given Correlation Coefficient Differs Significantly from Zero (lower triangle).**

Variable	F1	F2	F3	F5	F8	F10	F12
F1		0,969	0,451	0,347	0,782	0,190	
F2	$p \leq 0,001$		0,250	0,225	0,787		
F3	$p \leq 0,001$	$p \leq 0,006$		0,718	0,310	0,712	0,368
F5	$p \leq 0,001$	$p \leq 0,013$	0,001			0,230	
F8	$p \leq 0,001$	0,0000	$p \leq 0,001$	$p \leq 0,051$			
F10	$p \leq 0,037$	0,8802	$p \leq 0,001$	$p \leq 0,011$	$p \leq 0,059$		0,224
F12	$p \leq 0,546$	0,7030	$p \leq 0,001$	$p \leq 0,233$	$p \leq 0,961$	$p \leq 0,014$	

The method's fitting error  $\phi^2 = 0.9012\%$  is very small. This indicates that the selected diagnostic features are "collinear," meaning that formula (4) serves as a model for assessing the quality level of EDOF lenses.

The essence of this model is that we have obtained a single variable – a numerical measure – that is assigned to each operated eye, determining the quality level of the implanted EDOF lens. This measure allows for ranking the studied eyes post-surgery based on the quality of the applied EDOF lens. The values of this measure, calculated for 10 operated eyes, can be found in Table 6.

**Table 6: Values of the Synthetic Diagnostic Function  $Z_{PJS}$  Determined for 7 Features from  $F_1$  to  $F_{12}$  for the First Pairs of Eyes in the Study Group, as well as the Directions of Influence of the Diagnostic Features on the  $Z_{PJS}$  Level and the Method's Fitting Error  $\phi^2$ .**

No	F1	F2	F3	F5	F8	F10	F12	$Z_{PJS}$
Directions influence	-	-	-	-	-	-	-	$\phi^2 = 0,0090$
1	430	410	148	112	334	28	13	0,2727
2	182	153	99	47	119	51	21	0,5485
3	229	164	160	88	162	56	37	0,3173
4	208	164	127	67	143	64	35	0,3815
5	360	281	224	164	231	80	70	0,1163
6	490	481	97	5	221	32	71	0,3336
7	165	152	63	37	76	7	32	0,7415
8	231	224	57	18	111	25	4	0,8001
9	224	140	175	89	140	121	11	0,3945
10	220	130	180	95	152	153	16	0,3339

### Quality Characteristics of EDOF Lenses

Let us note that in model (4), the variable  $F_7$  – spherical aberration measured in diopters – does not appear. This is not accidental; when an EDOF lens is implanted, ex definitione, the patient should see without correction for this aberration, so it is not a diagnostic feature that affects the quality of the lens. Furthermore, in model (4), with the variable  $F_7$  included, the result showed that the weight of this variable does not differ significantly from zero.

To determine the quality values of EDOF lenses for the remaining types of aberrations, namely C, Z, and N, we use equation (4) for the estimators  $b_0, b_1, b_2, \dots, b_7$  with values presented in Table 1, replacing the values of variable F for each patient with the corresponding values of variables C, Z, and N.

The results of the comparisons of the mean  $Z_{PJS}$  quality levels for both types of EDOF lenses, presented in Table 7 and illustrated in Figure 2, indicate that the LUXSMART EDOF lens is characterized by a higher  $Z_{PJS}$  quality level than the VIVITY EDOF lens for the aberration type denoted by the symbol N.

**Table 7: Mean Values with SD for the Different Types of Aberrations, Divided by the Type of EDOF Lens Used.**

Aberration type	EDOF lens type		p test result
	VIVITY N = 68	LUXSMART N = 53	
ZF	$0,4804 \pm 0,1993$	$0,5166 \pm 0,2175$	0,288
ZC	$0,5284 \pm 0,2122$	$0,5433 \pm 0,2194$	0,610
ZZ	$0,522 \pm 0,2073$	$0,5743 \pm 0,2301$	0,127
ZN	$0,6897 \pm 0,2547$	$0,7988 \pm 0,2064$	0,033

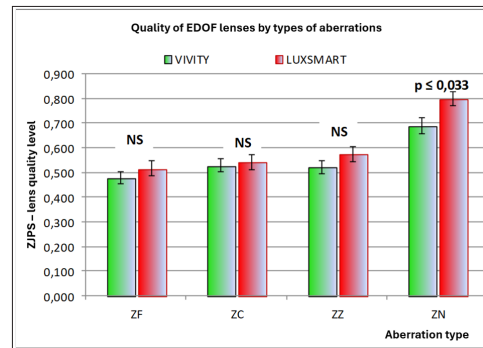


**Figure 2:** Shows a Comparison of the Mean  $Z_{PJS}$  Values—the Quality of EDOF Lenses with Standard Errors (SE) for Two Types of EDOF Lenses Used Across 4 Types of Aberrations. NS Indicates no Statistically Significant Difference.

### Discussion

Patient interest in reducing their reliance on glasses has fueled innovation in intraocular lens technology, prompting the arrival of extended depth of focus IOLs on the market [27]. According to the standards set by ANSI/AAO, EDOF IOLs aim to endow patients with enhanced distance-corrected intermediate vision and a broader depth of focus while maintaining best-corrected distance vision on par with traditional monofocal lenses [28,29]. However, it's noteworthy that these criteria do not specifically address the incidence of visual disturbances. Over the last ten years, the introduction of various EDOF optical technologies has diversified clinical outcomes and the extent of associated visual disturbances.

Using wavefront-shaping technology represents a significant advancement in ophthalmic surgery. When combined with a

thorough patient evaluation, this technology has the potential to notably enhance the visual quality for patients receiving IOL implants.

In summary, our analysis found that both Vivity and LuxSmart IOLs showed similar vision quality in terms of intraocular aberrations following cataract surgery, except for a minor increase in spherical aberrations with Vivity IOLs. The clinical impact of this increase may lead to minor differences in visual quality, particularly noticeable in specific conditions such as low-light environments.

Our analyzed sample demonstrates a notable tendency for a gender disparity, with females constituting 63.64% over males 36.36%. This indicates of a higher female prevalence aligning with epidemiological trends in cataract incidence [30].

Further evaluation through visual acuity testing and quality-of-life measures is necessary to gauge the subjective impact on patients' visual function. The lack of significant differences in other types of aberrations suggests that the choice between Vivity and LuxSmart IOLs can be influenced by criteria beyond aberration control, like IOL material properties, patient lifestyle, or surgeon preference.

Both Vivity and LuxSmart IOLs yield similar outcomes for most optical parameters post defocus correction. However, the notable increase in spherical aberrations with Vivity IOLs is a clinical consideration that may affect vision quality, especially in low-light conditions or while viewing complex patterns. Its clinical relevance hinges on individual patient experiences and impact on daily activities. The data, favoring Vivity IOLs in terms of the test wavefront beam diameter and CDVA, may not yield noticeable clinical benefits due to their small magnitudes. Given the lack of significant differences in key visual outcomes, the choice between Vivity and LuxSmart IOLs should consider patient-specific factors, surgeon preference, and cost-effectiveness. Additionally, lens design, material properties, and patient-reported outcomes should be part of the decision-making process when selecting the appropriate IOL for cataract patients.

Both Vivity and LuxSmart IOLs demonstrated similar postoperative outcomes in overall ocular aberrations, apart from a slight increase in spherical aberrations with Vivity IOLs. While this increase could have clinical implications, its significance should be interpreted carefully, considering the patient's specific visual needs. Overall, the largely equivalent performance of the two IOLs in most aberration categories indicates that lens choice should account for patient lifestyle, occupational visual demands, and surgery expectations. Ophthalmologists can confidently select either lens type, recognizing their similar visual acuity and refractive outcomes. While the increased aberrations with Vivity IOLs were statistically significant, their clinical impact would depend on individual patient sensitivity and the tolerance threshold of their visual system. Also Vivity showed a small but significant increase in the test wavefront beam's diameter with a minuscule improvement in logMAR, these differences were likely clinically unimportant. By using the Kreft model and taking into account empirical data, it was shown that both lenses generate similar levels of aberration.

The limitations in UNVA for patients with Vivity and LuxSmart IOLs are linked to the lenses' restricted depth of focus. Yet, their potential for fostering spectacle independence could play a crucial role in achieving satisfactory visual function across various lighting and distances. This adaptation, similar to neuroadaptation in multifocal lenses, may involve a time-intensive process activating various cortical areas responsible for attention, learning, cognitive control, and task objectives [31].

HOA variations are known to be pupil size-dependent. Our study utilized physiological pupil diameters under scotopic conditions, but individual responses can vary due to factors like ocular conditions, medication, age, and genetics. Participants showed differences in pupil sizes, which could impact HOA measurements and require further exploration. Surgeons should consider pupil size when choosing EDoF IOLs for their patients.

One limitation involves the difference between our assessment of human vision and aberrometers, which only rely on monochromatic measurements. Another limitation is the lack of standardization of aberrations and ocular metrics among the subjects as the heterogeneity of the studied group's corneal anatomy.

The achieved spherical equivalent refraction in both groups is affected by the precision and accuracy of the intraocular lens (IOL) power calculation algorithms, relying on preoperative biometric data and potential postoperative changes in corneal refractive power [32-36].

## References

1. Alio JL, Plaza-Puche AB, Fernández-Buenaga R, Pikkel J, Maldonado M. Multifocal intraocular lenses: An overview. *Surv. Ophthalmol.* 2017; 62: 611-634.
2. Breyer DRH, Beckers L, Ax T, Kaymak H, Klabe K, et al. Aktuelle Übersicht: Multifokale Linsen und Extended-Depth-of-Focus-Intraokularlinsen [Current Review: Multifocal Intraocular Lenses and Extended Depth of Focus Intraocular Lenses]. *Klin. Monbl. Augenheilkd.* 2020; 237: 943-957.
3. Niazi S, Gatziosas Z, Dhubhghaill SN, Moshirfar M, Faramarzi A, et al. Association of Patient Satisfaction with Cataract Grading in Five Types of Multifocal IOLs. *Adv. Ther.* 2024; 41: 1774.
4. Galvis V, Escaf LC, Escaf LJ, Tello A, Rodríguez LD, et al. Visual and satisfaction results with implantation of the trifocal Panoptix® intraocular lens in cataract surgery. *J. Optom.* 2022; 15: 219-227.
5. Lubiński W, Podboraczyńska-Jodko K, Kirkiewicz M, Mularczyk M, Post M. Comparison of visual outcomes after implantation of AtLisa tri 839 MP and Symfony intraocular lenses. *Int. Ophthalmol.* 2020; 40: 2553-2562.
6. Ang RET. Long-term trifocal toric intraocular lens outcomes in Asian eyes after cataract surgery. *J. Cataract. Refract. Surg.* 2023; 49: 832-839.
7. Karam M, Alkhawaiter N, Alkhabbaz A, Aldubaikhi A, Alsaif A, et al. Extended Depth of Focus Versus Trifocal for Intraocular Lens Implantation: An Updated Systematic Review and Meta-Analysis. *Am. J. Ophthalmol.* 2023; 251: 52-70.

8. Bellucci R, Morselli S, Pucci V. Spherical aberration and coma with an aspherical and a spherical intraocular lens in normal age-matched eyes. *J. Cataract. Refract. Surg.* 2007. 33: 203-209.
9. Werner W, Roth EH. Image properties of spherical as aspheric intraocular lenses. *Klin. Mon. Augenheilkd.* 1999. 214: 246-250.
10. Charman WN, Montés-Micó R, Radhakrishnan H. Problems in the measurement of wavefront aberration for eyes implanted with diffractive bifocal and multifocal intraocular lenses. *J. Refract. Surg.* 2008. 24: 280-286.
11. Fernández J, Rocha-de-Lossada C, Rodríguez-Vallejo M. Objective Optical Quality With Multifocal Intraocular Lenses Should Stop to Be Used or Cautiously Interpreted. *Asia Pac. J. Ophthalmol.* 2022. 11: 569.
12. Vega F, Faria-Ribeiro M, Armengol J, Millán MS. Pitfalls of Using NIR-Based Clinical Instruments to Test Eyes Implanted with Diffractive Intraocular Lenses. *Diagnostics* 2023. 13: 1259.
13. D’Oria F, Scotti G, Sborgia A, Boscia F, Alessio G. How Reliable Is Pyramidal Wavefront-Based Sensor Aberrometry in Measuring the In Vivo Optical Behaviour of Multifocal IOLs. *Sensors* 2023. 23: 3534.
14. Kass NE, Faden RR, Angus DC, Morain SR. Making the Ethical Oversight of All Clinical Trials Fit for Purpose. *JAMA*. 2025. 333:75-80.
15. Morris MC, Nelson RM. Randomized Controlled Trials as Minimal Risk: An Ethical Analysis. *Critical Care Medicine*. 2007. 35: 940-944.
16. Monach PA, Branch-Elliman W. Reconsidering ‘Minimal Risk’ to Expand the Repertoire of Trials With Waiver of Informed Consent for Research. *BMJ Open*. 2021. 11: e048534.
17. Woodward B. Challenges to Human Subject Protections in US Medical Research. *JAMA*. 1999. 282: 1947-1952.
18. Borkenstein AF, Borkenstein EM, Luedtke H, Schmid R. Optical Bench Analysis of 2 Depth of Focus Intraocular Lenses. *Biomed Hub*. 2021. 6: 77-85.
19. Siatiri H, Mohammadpour M, Gholami A, Ashrafi E, Siatiri N, et al. Optical aberrations, accommodation, and visual acuity with a bioanalogic continuous focus intraocular lens after cataract surgery. *J. Curr. Ophthalmol.* 2017. 29: 274-281.
20. Jun I, Choi YJ, Kim EK, Seo KY, Kim T. Internal spherical aberration by ray tracing-type aberrometry in multifocal pseudophakic eyes. *Eye*. 2012. 26: 1243-1248.
21. Thibos LN. Principles of Hartmann-Shack aberrometry. *J. Refract. Surg.* 2000. 16: 563-565.
22. Charman WN, Montés-Micó R, Radhakrishnan H. Problems in the measurement of wavefront aberration for eyes implanted with diffractive bifocal and multifocal intraocular lenses. *J. Refract. Surg.* 2008. 24: 280-286.
23. Rozema JJ, Van Dyck DE, Tassignon MJ. Clinical comparison of 6 aberrometers. Part 1: Technical specifications. *J. Cataract Refract. Surg.* 2005. 31: 1114-1127.
24. Plaza-Puche AB, Salerno LC, Versaci F, Romero D, Alio JL. Clinical evaluation of the repeatability of ocular aberrometry obtained with a new pyramid wavefront sensor. *Eur. J. Ophthalmol.* 2019. 29: 585-592.
25. Krefft A, Galanc T, Pandel W. Models of non-observable variables. *Systems: J. of transdisc. systems science*. 2004. 9: 34-48.
26. Krefft A, Galanc T, Filipowski H. On some methodological aspect of the life quality measurement. *Operations Research and Decisions*. 2003. 1: 19-30.
27. Kohnen T, Suryakumar R. Extended depth-of-focus technology in intraocular lenses. *J Cataract Refract Surg.* 2020. 46: 298-304.
28. Schwiegerling J, Gu X, Hong X, Lemp-Hull J, Merchea M. Optical principles of extended depth of focus IOLs. 2020.
29. American National Standard for Ophthalmics. American National Standard for Ophthalmics - Extended depth of focus intraocular lenses. 2018.
30. Shu Y, Shao Y, Zhou Q, Lu L, Wang Z, et al. Changing Trends in the Disease Burden of Cataract and Forecasted Trends in China and Globally from 1990 to 2030. *Clin Epidemiol*. 2023. 15: 525-534.
31. Rosa AM, Miranda AC, Patricio M, McAliden, C, Silva FL, et al. Functional Magnetic Resonance Imaging to Assess the Neurobehavioral Impact of Dysphotopsia with Multifocal Intraocular Lenses. *Ophthalmology* 2017. 124: 1280-1289.
32. Norrby S. Sources of error in intraocular lens power calculation. *J. Cataract. Refract. Surg.* 2008. 34: 368-376.
33. Langenbucher A, Szentmáry N, Cayless A, Bolz M, Hoffmann P, et al. Prediction of spectacle refraction uncertainties with discrete IOL power steps and manufacturing tolerances according to ISO using a Monte Carlo model. *Br. J. Ophthalmol.* 2023. 1: 8.
34. Langenbucher A, Hoffmann P, Cayless A, Bolz M, Wendelstein J, et al. Impact of uncertainties in biometric parameters on intraocular lens power formula predicted refraction using a Monte-Carlo simulation. *Acta Ophthalmol.* 2023. 1-11.
35. Kugelberg M, Lundström M. Factors related to the degree of success in achieving target refraction in cataract surgery: Swedish National Cataract Register study. *J. Cataract. Refract. Surg.* 2008. 34. 1935-1939.
36. Hill WE, Abulafia A, Wang L, Koch DD. Pursuing perfection in IOL calculations. II. Measurement foibles: Measurement errors, validation criteria, IOL constants, and lane length. *J. Cataract. Refract. Surg.* 2017. 43: 869-870.